

## Seismic interferometry with antipodal station pairs

Fan-Chi Lin<sup>1</sup> and Victor C. Tsai<sup>1</sup>

Received 25 June 2013; revised 19 August 2013; accepted 24 August 2013.

[1] In this study, we analyze continuous data from all Global Seismographic Network stations between year 2000 and 2009 and demonstrate that several body wave phases (e.g., PP, PcPPKP, SKSP, and PPS) propagating between nearly antipodal station pairs can be clearly observed without array stacking using the noise/coda cross-correlation method. Based on temporal correlations with global seismicity, we show that the observed body waves are clearly earthquake related. Moreover, based on single-earthquake analysis, we show that the earthquake coda energy observed between ~10,000 and 30,000 s after a large earthquake contributes the majority of the signal. We refine our method based on these observations and show that the signal can be significantly improved by selecting only earthquake coda times. With our improved processing, the PKIKP phase, which does not benefit from the focusing effect near the antipode, can now also clearly be observed for long-distance station pairs. **Citation:** Lin, F.-C., and V. C. Tsai (2013), Seismic interferometry with antipodal station pairs, *Geophys. Res. Lett.*, 40, doi:10.1002/grl.50907.

### 1. Introduction

[2] Seismic interferometry or ambient noise cross correlation has now routinely been used to extract travel-time information between two stations and applied to study interior earth structure [Breguier *et al.*, 2007; Moschetti *et al.*, 2010; Lin *et al.*, 2011]. While extracting surface waves is still the major application [e.g., Shapiro *et al.*, 2005; Yao *et al.*, 2006; Lin *et al.*, 2008], several recent studies have also shown that extracting deep-penetrating body waves using seismic interferometry is possible [Poli *et al.*, 2012; Lin *et al.*, 2013; Nishida 2013; Boué *et al.*, 2013]. The body wave phases, however, remain relatively weak and array stacking techniques are needed to strengthen the signals. Different source mechanisms, such as oceanic seismic hum [Nishida, 2013] and earthquake coda [Lin *et al.*, 2013], have been proposed to explain the observation of body waves in noise cross correlations.

[3] In this study, we demonstrate that deep-penetrating body wave phases propagating between the two stations can be extracted using seismic interferometry without array stacking. Specifically, we show that clear body wave signals can be observed in noise cross correlations [Bensen *et al.*, 2007] of nearly antipodal Global Seismographic Network

(GSN) station pairs [Figure 1a; Butler *et al.*, 2004] using ~9 years of data. At the antipode, many body wave phases (e.g., PP, PcPPKP, and SKSP; Figure 1b) tend to amplify due to geometrical focusing, which has long been observed in earthquake studies [Rial and Cormier, 1980; Butler and Tsuboi, 2010]. Based on the temporal variability of the signals, we show that the presence of these deep-penetrating phases is clearly earthquake related, consistent with our earlier study [Lin *et al.*, 2013]. Moreover, based on single-earthquake analysis, we show that coda energy excited by large earthquakes is the main contributor to the observed body waves. The coda energy is excited by large earthquakes through a number of different wave processes such as scattering, reflection, refraction, and diffraction and can be considered as semidiffusive [Aki, 1969; Campillo and Paul 2003]. We show that by only using the coda energy between 10,000 and 30,000 s after large earthquakes, the observed body wave signals can be considerably improved. The observation of a clear PKIKP phase, which is not affected strongly by geometrical focusing, demonstrates the potential to significantly improve the existing path coverage for deep earth study [e.g., Morelli *et al.*, 1986; Sun and Song, 2008].

### 2. Data and Results

[4] We closely follow the method described by Bensen *et al.* [2007] and Lin *et al.* [2008] to obtain traditional vertical-vertical ambient noise cross correlations using continuous data between year 2000 and 2009 for all available GSN stations. This method uses temporal normalization (using the running-absolute-mean over a 128 s time window of the 15 to 50 s bandpassed raw noise waveform) to suppress impulsive high-amplitude earthquake signals. While the temporal normalization process also slightly suppresses earthquake coda to the ambient noise level, no further processing is used to reduce earthquake contributions. Spectral whitening is also applied to flatten the amplitude spectrum between a 5 and 800 s period before cross correlation.

#### 2.1. Noise Cross Correlations and Body Wave Phases

[5] In this study, we focus our analysis on nearly antipodal station pairs. The noise cross correlations for the five GSN pairs that are closest to 180° separation are shown in Figure 1c. The body wave phases including PP, PcPPKP, and SKSP (Figure 1b) can be clearly observed on both positive and negative time lags for station pairs PAB-SNZO and BBSR-NWAO, where the station separations are within 2° from being antipodal. These body wave phases are mostly absent for the station pairs MBWA-SJG, KBS-SBA, and KIP-TSUM, where the stations are slightly farther away (>4°) from their respective antipodal locations. The observation of these body waves and the dependency on station separation closely resembles the classic study of Rial and Cormier [1980] based on the 1968 New Zealand Inangahua

Additional supporting information may be found in the online version of this article.

<sup>1</sup>Seismological Laboratory, Division of Geological and Planetary Sciences, California Institute of Technology, Pasadena, California, USA.

Corresponding author: F.-C. Lin, Seismological Laboratory, Division of Geological and Planetary Sciences, California Institute of Technology, Pasadena, CA 91125, USA. (linf@caltech.edu)

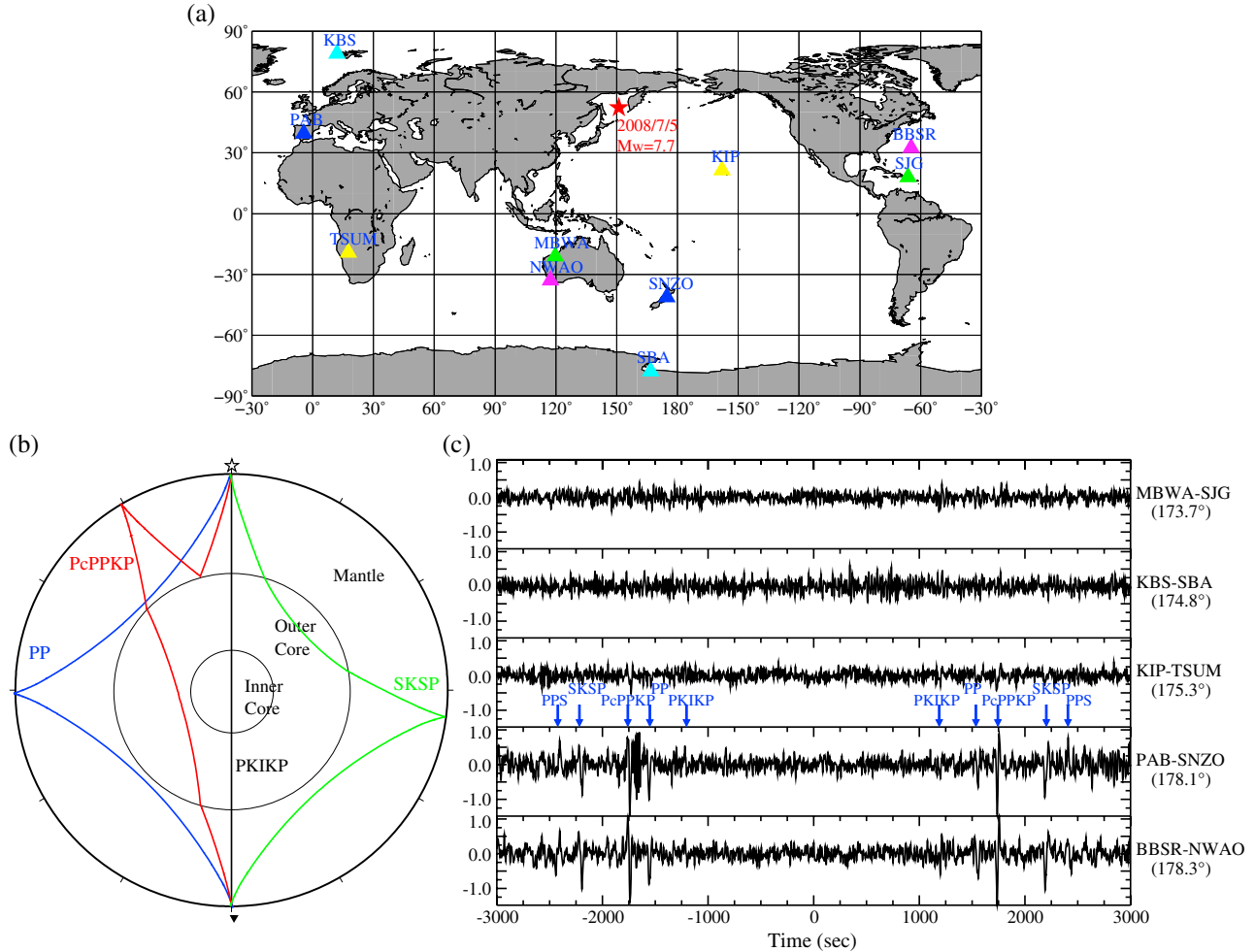


**Figure 1.** Ambient noise cross correlations for five nearly antipodal GSN station pairs. (a) The triangles mark the locations of the GSN stations used in this paper, with antipodal pairs colored the same. The star shows the location of the 5 July 2008  $M_w$  7.7 Sea of Okhotsk earthquake used in Figures 2 and 3. (b) Schematic plot of the PKIKP (black), PP (blue), PcPPKP (red), and SKSP (green) raypaths. The star and filled triangle denote source and receiver locations, respectively. (c) The observed broadband ambient cross correlations sorted by distance. Several observed body wave phases are indicated.

earthquake. Note that the PKIKP phase does not benefit from the focusing effect at the antipode and is only weakly observed.

[6] The observation of strong body wave phases for antipodal station pairs provides a unique opportunity to better understand the source of the cross-correlation signals. In particular, we can now examine the correlation between strong body waves and global seismicity without array stacking [Lin *et al.*, 2013]. To strengthen the signals and suppress noise, all further cross correlations shown are low-passed with a 10 s corner period and are symmetric-component cross correlations with positive and negative time lags stacked together.

[7] Figure 2a shows cross correlations for the BBSR-NWAO station pair stacked by days with earthquakes above a given magnitude threshold (i.e., all days,  $M_w > 6.3$ ,  $M_w > 7.0$ ,  $M_w > 8.0$ , and 5 July 2008 single day) in the Global Centroid Moment Tensor (CMT) Catalog [Ekström *et al.*, 2012]. Clear body wave signals are observed in all cases even for the single-day cross correlation of 5 July 2008, when a  $M_w$  7.7 deep earthquake happened beneath the Sea of Okhotsk (~636 km in depth; Figure 1a). Despite the significant reduction in the number of days, from 2454 days in total to 435 and 93 days, when the  $M_w > 6.3$  and  $M_w > 7.0$

selection criteria are used, the amplitude of the body waves is only reduced by a factor of 2 and 4, respectively. Because the noise level of a cross correlation is generally proportional to the square root of the total time duration used, the  $M_w > 6.3$  and  $M_w > 7.0$  stacks actually have slightly higher signal-to-noise ratios compared with the 'all days' stack because of lower noise levels. These observations suggest that the ambient noise contribution (without earthquake coda, e.g., due to ocean microseism) to the body wave observation is likely to be small and including all ambient noise signals can contribute negatively to the overall signal-to-noise ratio. On the other hand, the factor of ~10 amplitude decrease from  $M_w > 7.0$  to  $M_w > 8.0$  is on the same order as the reduction in the number of days, suggesting that the largest earthquakes do not necessarily contribute more. This is probably because the largest earthquakes tend to be shallower and therefore excite more surface waves than body waves.

[8] To further demonstrate the correlation between the observed body waves and global seismicity, in Figure 2b, we plot a histogram of all the daily cross-correlation amplitudes at a lag time of 1736 s for the BBSR-NWAO station pair. This lag time corresponds to the observed arrival of

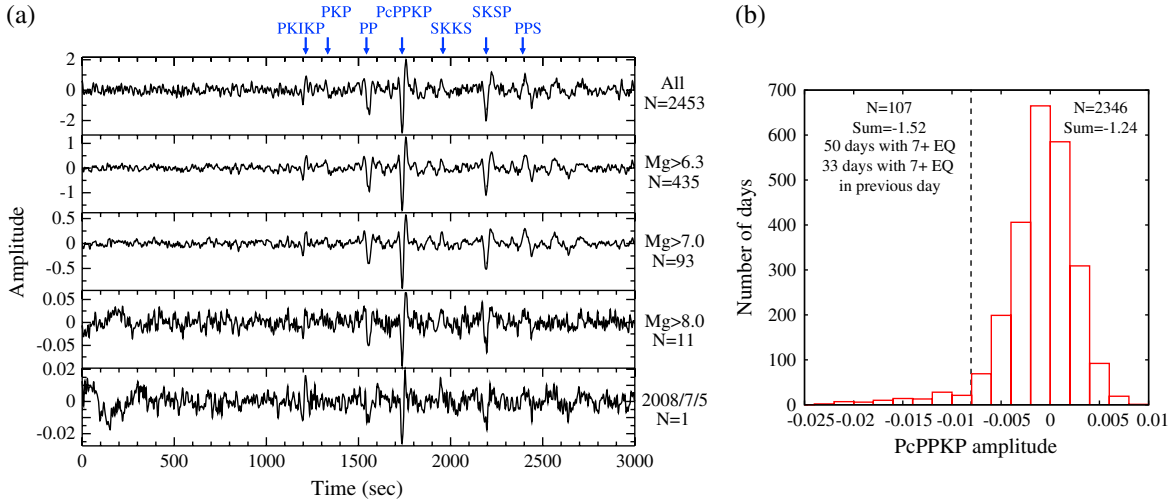


**Figure 2.** Correlation between the observed core phases and global seismicity. (a) The cross correlations between BBSR and NWA0 from stacking different numbers of days. The selection criterion and the total number of days included are indicated on the right. Several observed body wave phases are indicated. (b) The distribution of the daily cross-correlation amplitudes at 1736 s lag time. A dashed line at an amplitude of  $-0.008$  is shown that separates the Gaussian-like distribution on the right from the flatter distribution on the left. The total number of days and the summed amplitude for the two distributions are indicated.

PcPPKP [Rial and Cormier 1980], which is the strongest phase observed for the nearly antipodal station pair (Figure 2a), and the phase has a negative amplitude in the vertical-vertical cross correlations. Two regions with very different distributions are observed above and below an amplitude of  $-0.008$  (Figure 2b). (Note that these amplitudes have arbitrary units due to the temporal and spectral normalizations but can be compared with the  $\sim 0.0025$  rms noise level of each daily cross correlation.) Above an amplitude of  $-0.008$ , a Gaussian-like distribution centered slightly below zero with a width of  $\sim 0.0025$  is observed, and contains over 95% of the days we analyzed. Below  $-0.008$ , on the other hand, a relatively flat distribution is observed. Despite this flat part of the distribution containing only  $\sim 4\%$  of the days we analyzed (107 out of 2453 days), it contributes to more than half of the PcPPKP amplitude observed in the full stacked cross correlation shown in Figure 2a (top panel). Comparing the days within the flat region with global seismicity [Ekström *et al.*, 2012] reveals that, out of the 107 days, there are 50 days with earthquakes  $M_w > 7.0$  and 33 days with earthquakes  $M_w > 7.0$  on the previous day. Note that there are 93 days in total with  $M_w > 7.0$  out of the entire 2346 days we studied. This correlation suggests that the observation of body waves in our noise cross correlations is likely due to constructive interference of earthquake coda energy, which potentially lasts for hours after large earthquakes. Similar observation can be made for another nearly antipodal station pair PAB-SNZO, where occurrences of large PcPPKP amplitudes are highly correlated with the times for which BBSR-NWA0 also has large PcPPKP amplitudes (Figure S1 in the supporting information).

## 2.2. Coda Cross Correlation

[9] To demonstrate that the earthquake coda, rather than the early-arriving earthquake body waves, contributes most to the observed body waves, we analyze the temporal variation of the cross correlation for the BBSR-NWA0 station pair for 5 July 2008. On that day, the  $M_w$  7.7 Sea of Okhotsk

earthquake happened around 2:12 A.M. UTC time [Ekström *et al.*, 2012; Figure 1a]. Figure 3a shows the raw waveforms and the waveforms after the temporal and spectral normalization for stations BBSR and NWA0. Note that running-absolute-mean amplitudes of 15–50 s bandpassed waveforms are used to suppress the earthquake signal [Lin *et al.*, 2008]. While the temporal normalization process levels the waveform amplitude within the 15–50 s period band, the amplitude of the broadband waveform is not completely leveled (e.g., lower two panels of Figure 3a).

[10] We calculate cross correlations based on the normalized time series using three different time windows (Figure 3b). The 0–20,000, 20,000–40,000, and 40,000–60,000 s time windows of the day (UTC time) roughly contain the earthquake main phases, early earthquake coda, and late earthquake coda, respectively, with the earthquake origin UTC time being at  $\sim 8000$  s. As shown in Figure 3b, only the cross correlation using the early earthquake coda time window results in a clear PcPPKP phase. To further understand the evolution of the body wave signal, we also calculate the accumulated cross-correlation amplitudes at positive and negative 1736 s time lags (the expected PcPPKP arrival time) using a time window with a fixed zero starting time and a sliding ending time. A continuous increase in PcPPKP amplitude (i.e., cross-correlation amplitude becoming more negative) is observed for both positive and negative time lags between  $\sim 10,000$  and  $\sim 50,000$  s after the earthquake (Figure 3c), but the decrease is particularly strong between  $\sim 10,000$  and  $\sim 30,000$  s after the earthquake. The decreasing cross-correlation amplitude represents the continuous accumulation of PcPPKP energy propagating between the two stations after the earthquake. We consider this to be direct evidence that the continuous long-lasting coda energy excited by a large earthquake is partially diffusive, and that deep body wave seismic interferometry is best applied to this coda time period. In particular, we identify the coda time window between 10,000 and 30,000 s after a large earthquake as the most energetic time period for deep body wave seismic interferometry. Similar observations can be made using other

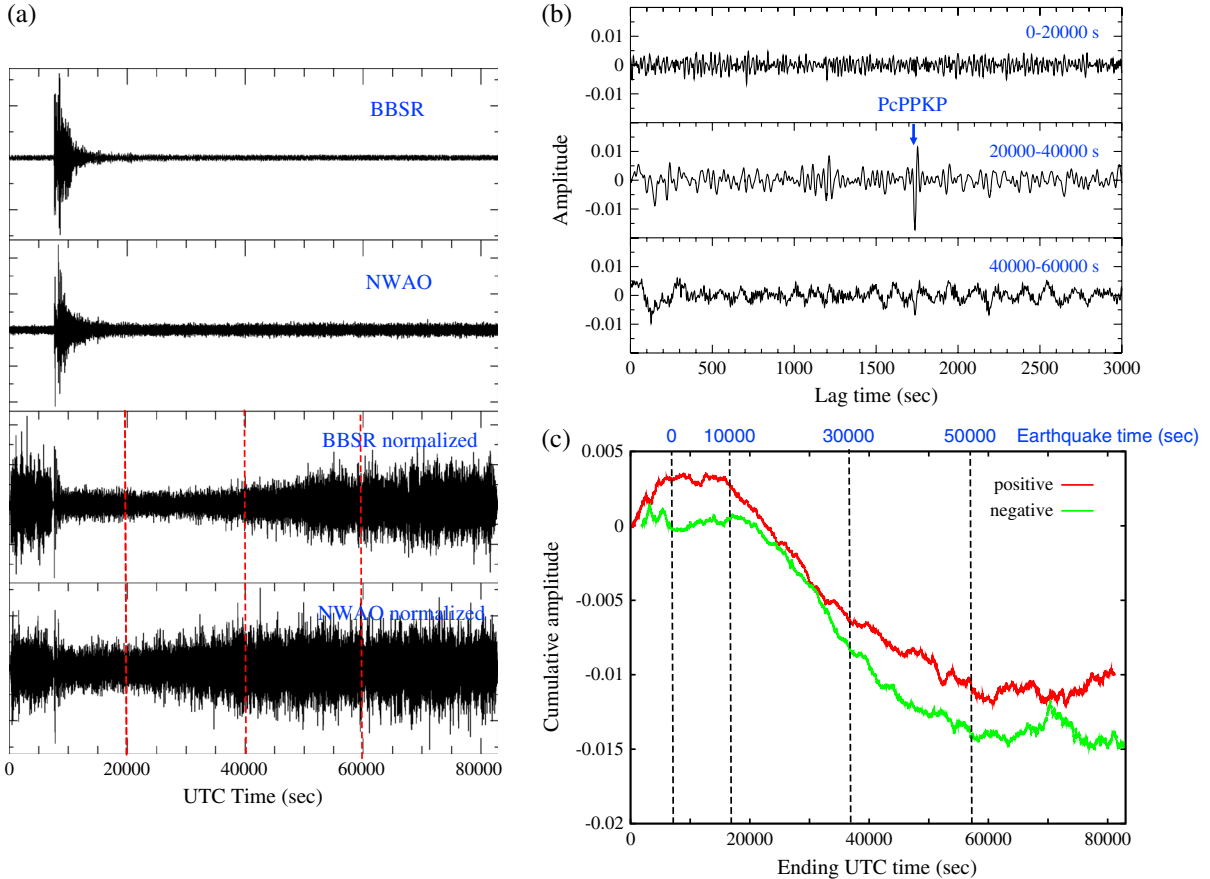


**Figure 3.** Temporal variability of the cross correlation for a single earthquake. (a) The raw and temporally normalized waveforms observed at stations BBSR and NWAQ on 5 July 2008. Clear signals due to the  $M_w$  7.7 Sea of Okhotsk earthquake can be observed in the raw waveforms. The red dashed lines (bottom two panels) indicate the time windows used for the cross correlations shown in Figure 3b. (b) The cross correlations between BBSR and NWAQ using three different time windows. The arrow indicates the PcPPKP phase. (c) The cumulative amplitude of the cross correlation at negative (green) and positive (red) 1736 s lag time calculated based on a time window with fixed zero starting time and a sliding ending time. The black dashed lines indicate the time after the earthquake. Notice that the cumulative amplitude decreases continuously between  $\sim 18,000$  and  $\sim 58,000$  s UTC time, which corresponds to the time between  $\sim 10,000$  and  $\sim 50,000$  s after the earthquake.

earthquakes, both shallow and deep, and for other nearly antipodal station pairs (e.g., see Figures S2 and S3 in the supporting information). Note that the accumulation of body wave energy stops when the coda energy attenuates below the surface-wave dominated ambient noise or if a following event’s surface waves dominate the signals.

[11] The observation above naturally leads to the refinement of our seismic interferometry process to better extract deep propagating body waves. Specifically, we propose to include only the most energetic coda time windows after large earthquakes in the cross-correlation calculation. While an ‘all days’ stack includes the earthquake coda energy, it also includes many undesired noise signals and hence reduces the signal-to-noise level of the observed body waves.

[12] Figure 4 shows the cross correlations for the five station pairs shown in Figure 1 but only stacking time windows with earthquake coda energy. Here, we select all earthquakes larger than  $M_w$  7.0 in the Global CMT Catalog [Ekström *et al.*, 2012] and include all time series between 10,000 and 30,000 s after the earthquakes. The signal-to-noise ratio clearly improves compared to the original ambient noise cross correlations (Figure 1c), and now clear body wave phases (including PKIKP) can be observed at all five station

pairs. The ability to extract deep body wave phases such as PKIKP propagating between each permanent GSN station pair can potentially significantly improve data coverage for deep earth study. The fact that body waves traveling through the exact same paths can be repeatedly measured at different times may also potentially be useful for studying temporal variations in deep earth structure [e.g., Butler and Tsuboi, 2010].

### 3. Concluding Remarks

[13] The observed correlation between global seismicity and the strength of body wave phases in this study is generally consistent with our earlier result based on regional arrays using array stacking [Lin *et al.*, 2013]. This is perhaps not surprising considering that both studies focus on body waves that propagate through the deep earth. Quantifying the uncertainty in arrival times of body waves extracted by seismic interferometry, the importance of different wave processes (e.g., scattering, reflection, refraction, and diffraction) on coda generation, and the effect of earth heterogeneity on the body wave observations remain subjects of future contribution. Initial examination suggests that the observed body

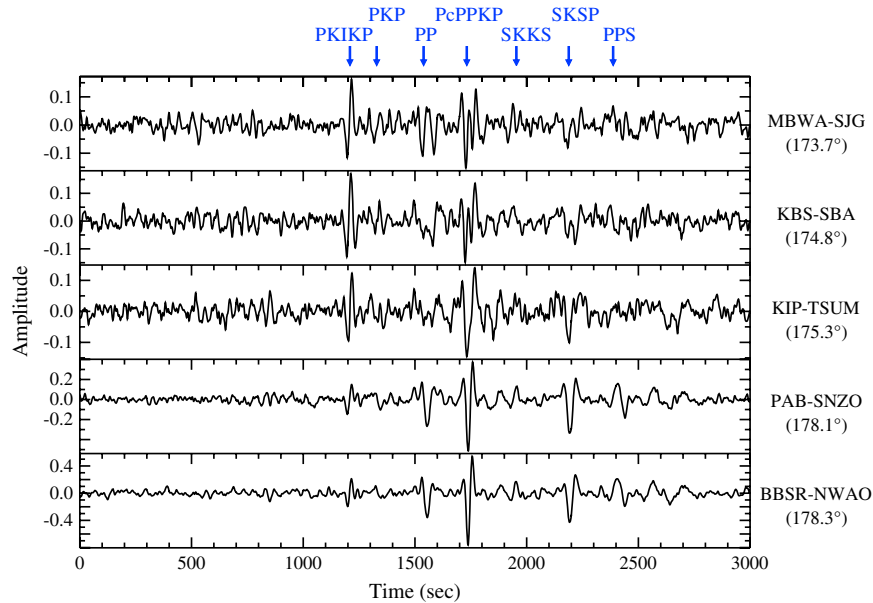


**Figure 4.** Earthquake coda cross correlations for the five nearly antipodal GSN station pairs shown in Figure 1. We use all earthquakes larger than  $M_w$  7.0 [Ekström *et al.*, 2012] that occurred between 2000 and 2009, and choose all times between 10,000 and 30,000 s after the earthquakes to cross-correlate. Note that temporal and spectral normalizations [Lin *et al.*, 2008] are applied before the cross correlation. Several observed body wave phases are indicated.

wave amplitudes are dependent on the earthquake magnitude but are not strongly dependent on the location and depth of earthquakes (Figures S1, S2, and S3 in the supporting information). While it remains unclear whether shallower body wave phases such as direct P and direct S can also be better extracted using earthquake coda, applying coda interferometry to calculate autocorrelations for GSN stations suggests that several core phases (e.g., ScS and PKIKP2; Figure S4 in the supporting information) can also be extracted without array stacking. This improvement can be particularly significant for extraterrestrial studies where the number of stations is limited [Weber *et al.*, 2011; <http://insight.jpl.nasa.gov/home.cfm>]. The ability to extract the ScS phase and determine its polarity using autocorrelation, for example, would provide direct evidence on the existence of a liquid outer core for extraterrestrial planets.

[14] **Acknowledgments.** The authors thank Xiaodong Song, Vernon F. Cormier, Rob W. Clayton, Donald V. Helmberger, and Zacharie Duputel for comments that helped to improve this paper. All data used in this paper were obtained from the IRIS-DMC. This work has been supported by the NSF grant EAR-1316348.

[15] The Editor thanks Xiaodong Song and an anonymous reviewer for their assistance in evaluating this paper.

## References

- Aki, K. (1969), Analysis of seismic coda of local earthquakes as scattered waves, *J. Geophys. Res.*, *74*, 615–631, doi:10.1029/JB074i002p00615.
- Bensen, G. D., M. H. Ritzwoller, M. P. Barmin, A. L. Levshin, F. Lin, M. P. Moschetti, N. M. Shapiro, and Y. Yang (2007), Processing seismic ambient noise data to obtain reliable broad-band surface wave dispersion measurements, *Geophys. J. Int.*, *169*, 1239–1260, doi:10.1111/j.1365-246X.2007.03374.x.
- Boué, P., P. Poli, M. Campillo, H. Pedersen, X. Briand, and P. Roux (2013), Teleseismic correlations of ambient seismic noise for deep global imaging of the Earth, *Geophys. J. Int.*, doi:10.1093/gji/ggt160.
- Brenguier, F., N. M. Shapiro, M. Campillo, A. Nercessian, and V. Ferrazzini (2007), 3-D surface wave tomography of the Piton de la Fournaise volcano using seismic noise correlations, *Geophys. Res. Lett.*, *34*, L02305, doi:10.1029/2006GL028586.
- Butler, R., and S. Tsuboi (2010), Antipodal seismic observations of temporal and global variation at Earth’s inner-outer core boundary, *Geophys. Res. Lett.*, *37*, L11301, doi:10.1029/2010GL042908.
- Butler, R., *et al.* (2004), Global seismographic network surpasses its design goal, *Eos Trans. AGU*, *85*(23), 225–229.
- Campillo, M., and A. Paul (2003), Long-range correlations in the diffuse seismic coda, *Science*, *299*, 547–549, doi:10.1126/science.1078551.
- Ekström, G., M. Nettles, and A. M. Dziewonski (2012), The global CMT project 2004–2010: centroid-moment tensors for 13,017 earthquakes, *Phys. Earth Planet. Inter.*, *200–201*, 1–9.
- Lin, F., M. P. Moschetti, and M. H. Ritzwoller (2008), Surface wave tomography of the western United States from ambient seismic noise: Rayleigh and Love wave phase velocity maps, *Geophys. J. Int.*, *173*, 281–298.
- Lin, F. C., M. H. Ritzwoller, Y. Yang, M. P. Moschetti, and M. J. Fouch (2011), Complex and variable crustal and uppermost mantle seismic anisotropy in the western United States, *Nat. Geosci.*, *4*, 55–61, doi:10.1038/ngeo1036.
- Lin, F.-C., V. C. Tsai, B. Schmandt, Z. Duputel, and Z. Zhan (2013), Extracting seismic core phases with array interferometry, *Geophys. Res. Lett.*, *40*, 1049–1053, doi:10.1002/grl.50237.
- Morelli, A., A. M. Dziewonski, and J. H. Woodhouse (1986), Anisotropy of the inner core inferred from PKIKP travel-times, *Geophys. Res. Lett.*, *13*, 1545–1548.
- Moschetti, M. P., M. H. Ritzwoller, F. Lin, and Y. Yang (2010), Seismic evidence for widespread crustal deformation caused by extension in the western USA, *Nature*, *464*, 885–889.
- Nishida, K. (2013), Global propagation of body waves revealed by cross-correlation analysis of seismic hum, *Geophys. Res. Lett.*, *40*, 1691–1696, doi:10.1002/grl.50269.
- Poli, P., M. Campillo, and H. Pedersen (2012), and LAPNET Working Group, Body-Wave Imaging of Earth’s Mantle Discontinuities from Ambient Seismic Noise, *Science*, *338*, 1063–1065, doi:10.1126/science.1228194.
- Rial, J. A., and V. F. Cormier (1980), Seismic waves at the epicenter’s antipode, *J. Geophys. Res.*, *85*, 2661–2668, doi:10.1029/JB085iB05p02661.
- Shapiro, N. M., M. Campillo, L. Stehly, and M. H. Ritzwoller (2005), High resolution surface wave tomography from ambient seismic noise, *Science*, *307*, 1615–1618.
- Sun, X. L., and X. D. Song (2008), Tomographic inversion for three-dimensional anisotropy of Earth’s inner core, *Phys. Earth Planet. Inter.*, *167*, 53–70, doi:10.1016/j.pepi.2008.02.011.
- Weber, R. C., P. Y. Lin, E. J. Garnero, Q. Williams, and P. Lognonne (2011), Seismic detection of the lunar core, *Science*, *331*, 309–312, doi:10.1126/science.1199375.
- Yao, H., R. D. van der Hilst, and M. V. de Hoop (2006), Surface-wave array tomography in SE Tibet from ambient seismic noise and two-station analysis – I. Phase velocity maps, *Geophys. J. Int.*, *166*, 732–744.